

Mapping graph state orbits under local complementation

Jeremy C. Adcock^{*1}, Sam Morley-Short¹, Axel Dahlberg², and Joshua W. Silverstone¹

¹Quantum Engineering Technology (QET) Labs, H. H. Wills Physics Laboratory & Department of Electrical & Electronic Engineering, University of Bristol, Merchant Venturers Building, Woodland Road, Bristol BS8 1UB, UK

²QuTech - TU Delft, Lorentzweg 1, 2628CJ Delft, The Netherlands

October 2019

Graph states, and the entanglement they posses, are central to modern quantum computing and communications architectures. Local complementation—the graph operation that links all local-Clifford equivalent graph states—allows us to classify all stabiliser states by the entanglement they posses. Here, we study the structure of the orbits generated by local complementation, mapping them up to 9 qubits and revealing a rich hidden structure. We observe correlations of these orbits’ properties, for example their colourability, with known entanglement metrics, such as Schmidt measure, and find relationships between an orbit’s connectivity and the entanglement of its graph states. We provide data for each of the 587 orbits up to 9 qubits as well as means to visualise them, uncovering their exquisite patterns. It is well known that graph theory and quantum entanglement have strong interplay—our exploration deepens this relationship, providing new tools with which to probe the nature of nonlocal stabiliser states.

1 Introduction

Graph states provide a language of entanglement between qubits and are at the core of modern quantum computing and communication architectures across all qubit platforms^{1–7}. All stabiliser states are local-Clifford (LC) equivalent[†] to a set of graph states¹⁰, and those graph states are related by repeated application of a simple graph operation, local complementation^{11,12}. Since local operations cannot change a state’s entanglement, graph states provide a way to classify all stabiliser states by the entanglement they posses.

Graph state entanglement is well studied^{11–15}, with each of the $\sim 1.6 \times 10^{12}$ non-isomorphic graph states up to 12 qubits classified into $\sim 1.3 \times 10^6$ inequivalent classes^{16,17}. There is a polynomial time algorithm to compute the local-Clifford (LC) unitary relating two graph states (if there is one)^{18,19}. In contrast, the problem of determining if a target graph state can be generated from an input graph state using LC operations, local Pauli measurements and classical communication (LC+LPM+CC) is NP-complete for both labelled^{14,20} and unlabelled graphs¹⁵. In graph theoretical nomenclature, this is equivalent to deciding if the target graph is a *vertex minor* of the input graph. Though NP-complete, this task has been shown to be fixed parameter tractable: the exponential part of the task’s complexity de-

pends on a graph-specific parameter, the rank width^{14,21}. It is also known that counting single-qubit Clifford equivalent graph states is #P-complete²².

Recently we showed that interspersing local complementations with CZ operations can lead to a reduction in CZ complexity²³. However, little is known about the structure of the orbits that are generated by local complementation. These orbits are themselves graphs, in which each orbit vertex represents a graph state and edges between them are induced by local complementation of different graph state vertices (see Fig. 1). Here, we refer to the object that links graphs via local complementation as their ‘orbit’, and we refer to those component graphs as ‘graph states’. These orbits, which are wildly complex, give a fresh perspective for the study of stabiliser entanglement and graph states, while providing new tools for optimising quantum protocols.

In this work, we map the space of graph states and their relationship via local complementation, generating the orbit of each of the 587 entanglement classes up to $n \leq 9$ qubits. We explicitly relate properties of these orbits to properties of their component graph states, and observe correlations between orbit parameters and Schmidt measure. We also plot an illustrative selection of these orbits, and identify promising avenues for both analysis and applications. All the data generated in this study are available online²⁴, together with a means to plot them.

2 Graph state orbits

Graph states are quantum states with a one-to-one correspondence to mathematical graphs^{11,12}. A graph, $G = (V, E)$, is a combinatoric object defined by a set of edges E between a set of vertices V . The corresponding graph state is written:

$$|G\rangle = \prod_{(i,j) \in E} \text{CZ}_{ij} |+\rangle^{\otimes |V|}. \quad (1)$$

Here, $|+\rangle = (|0\rangle + |1\rangle)/\sqrt{2}$ and $\text{CZ} = |00\rangle\langle 00| + |01\rangle\langle 01| + |10\rangle\langle 10| - |11\rangle\langle 11|$. Connected n -vertex graphs have genuine n -partite entanglement.

Remarkably, graph states can be locally equivalent, despite having different constructions via nonlocal CZ gates^{11,12}. Specifically, graphs are locally equivalent if and only if they can be transformed into one another by successive applications of local complementation.

Local complementation of a vertex α , LC_α , applied to a graph, $G(V, E)$, acts to complement the neighbourhood of the vertex α . That is, in the neighbourhood of α , it removes edges if they are present, and adds any edges are missing

^{*}jeremy.adcock@bristol.ac.uk

[†]Here, we use ‘local equivalent’ to describe LC equivalence and ‘entanglement class’ to describe sets of locally equivalent graphs. Note that states which are LC equivalent are also local unitary equivalent up to at most 27 qubits⁸, with a lower bound of 8 qubits⁹.

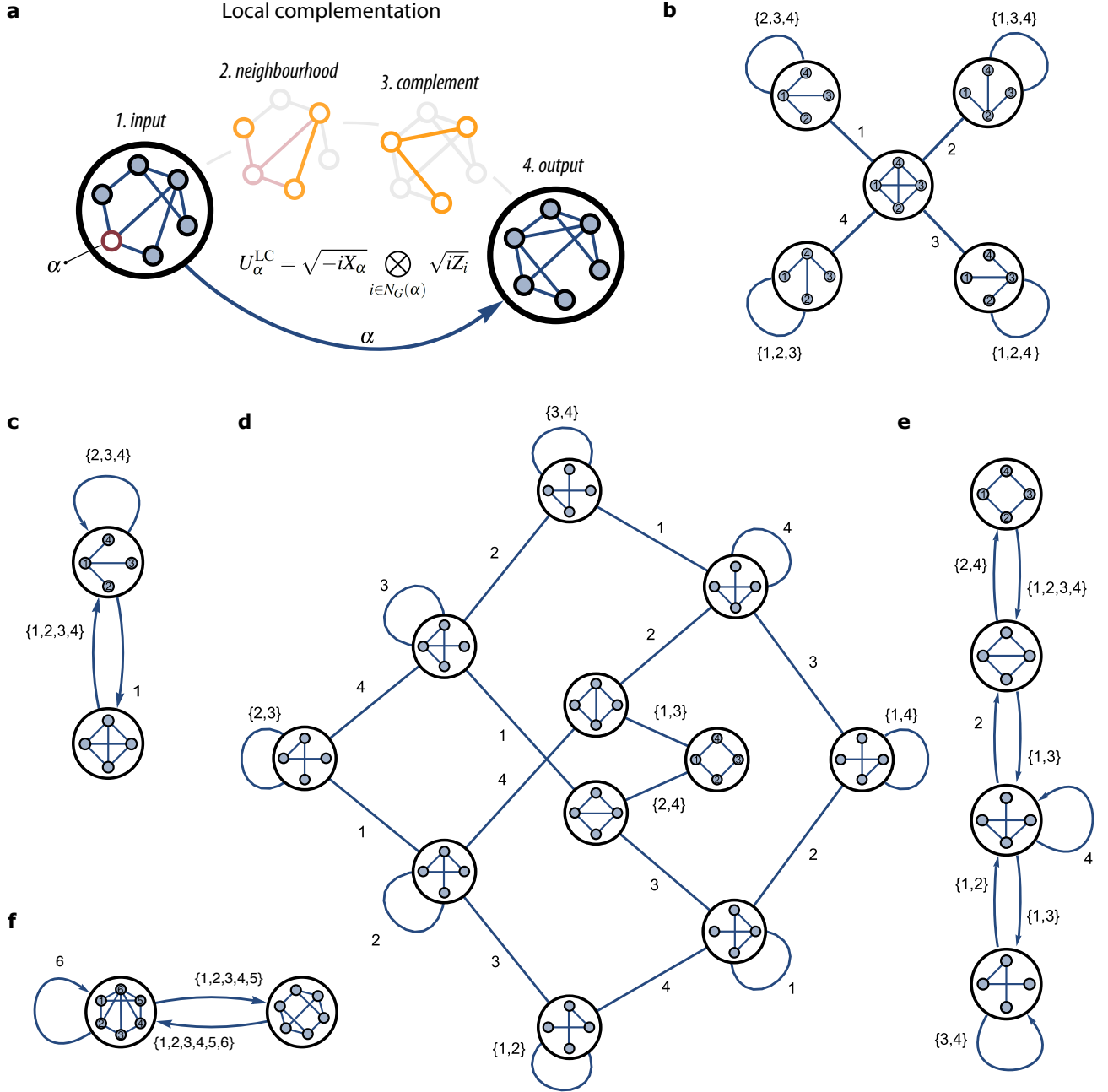


Fig. 1: Local complementation and its orbits. Orbit edges are labelled with the vertex that undergoes local complementation. **a.** A guide to local complementation. The neighbourhood of qubit α is complemented to yield the output graph. **b.** The orbit L_3 (GHZ entanglement of four qubits). **c.** The orbit C_3 , where isomorphic graph states are considered equal. **d.** The orbit L_4 (cluster state entanglement of four qubits). This is one of three equivalent orbits, which together contain every isomorphism of the contained graph states. **e.** The orbit C_4 . **f.** The orbit C_{19} . Graph state vertices are labelled descending clockwise from noon (see **b**). We use directed edges when drawing C_i orbits as only one isomorphism of the graph states can be drawn on an orbit.

(see Fig. 1a). More formally:

$$\text{LC}_\alpha(G(V, E)) \rightarrow G(V, E'), \quad (2)$$

where

$$E' = E \cup K_{N_G(\alpha)} - E \cap K_{N_G(\alpha)} = E \Delta K_{N_G(\alpha)}. \quad (3)$$

Here, $K_{N_G(\alpha)}$ is the set of edges of the complete graph on the vertex set $N_G(\alpha)$, the neighbourhood of α , and, Δ is the symmetric difference. On graph states, the following local

unitary implements local complementation^{11,12}:

$$U_\alpha^{\text{LC}} = \sqrt{-iX_\alpha} \bigotimes_{i \in N_G(\alpha)} \sqrt{iZ_i} \quad (4)$$

Where $U_\alpha^{\text{LC}}|G\rangle = |\text{LC}_\alpha(G)\rangle$. Repeated application of local complementation is guaranteed to hit every member of an entanglement class of locally equivalent graph states, given any member of that class as a starting point^{11,12}. This defines graph (and therefore stabiliser) entanglement classes, each

with their own orbit under local complementation. So far, these classes have been uniquely specified¹⁷ up to $n = 12$, while the structure of the orbits generated by local complementation has not yet been studied.

All n -vertex graphs can be locally complemented in n different ways, generating up to n different graphs. Each of these can be locally complemented further, generating up to $n - 1$ new graphs (local complementation is self inverse). We can repeatedly local complement graphs until we find no new ones, concluding that all graphs in the class have been found. By performing every local complementation on every graph in the class, the orbit is mapped (see Section 2.3). We will denote these orbits L_i for entanglement class i , canonically indexed as in ref. 17.

This orbit is itself naturally represented as a graph—its vertices are graph states and the edges that link them are local complementations on the graph state’s vertices (see Fig. 1). Edges of the orbits are labelled with a vertex index indicating which local complementation links the two graph states on the orbit vertices. Since local complementation is self-inverse, these edges are undirected. Some simple examples of orbits are shown in Figs. 1b,d.

2.1 A quantum Rubik’s cube

Local complementation orbits have an entertaining analogy with a Rubik’s cube (a popular puzzle toy). Each face of a Rubik’s cube is a different colour, which is itself separated into $3 \times 3 = 9$ individual squares. This is the cube’s solved state. The toy has 6 basic moves, which rotate the different faces of the cube by 90° . By applying these six moves in a random combination, a random state of the cube is generated. The challenge is then to return the cube to its solved state. For a mathematician, the challenge is to understand the cube’s symmetry, and solve it in the general case.

Using about one billion seconds (35 years) of CPU time, the Rubik’s cube Cayley graph—the orbit of the states of the cube—has been computed²⁵. Indeed, a Rubik’s cube has $\sim 4.3 \times 10^{19}$ states and its orbit has diameter 26. That is, any Rubik’s cube can always be solved in 26 90° moves or less (20 moves if either 90° or 180° rotations are allowed). ‘Cubers’, as Rubik’s cube aficionados are known, call 26 ‘god’s number’.

In our analogy, the many states of the toy are our graph states, and rotating the different faces of the cube corresponds to local complementation of different graph vertices. As evidenced by the ratio of its cardinality to its diameter ($\sim 10^{18}$), the orbit of the Rubik’s cube is highly dense (though each vertex only has six edges). Each of the ~ 1.3 million entanglement classes of 12 qubits has its own unique orbit—each of them is another Rubik’s cube (with 12 rather than 6 moves). Note there are factorially many entanglement classes as n is increased. God’s number (the orbit diameter) for local complementation orbits depends on the class. Using about a week of CPU time on a standard desktop computer, we compute the diameter of local complementation is maximally 9 for 9-qubit graph states. That is, any two locally equivalent graph states are at most 9 local complementations distant from one another).

2.2 Isomorphic graph states

Graphs can be symmetric under relabelling of their vertices—such graphs are said to be *isomorphic*. Graph states which are isomorphic share the same variety of entanglement. This is an important feature for the implementation of protocols where qubit relabelling is non-trivial—this includes most quantum information processing and communication scenarios. Here we consider both cases. We denote orbits C_i when isomorphic graphs are considered equal (unlabelled graph states), and L_i otherwise (labelled graph states). C_i contain on average $1/8$ as many graph states as their partner L_i orbits for $n < 9$ qubits. This greatly reduces the computational resources needed to map and analyse them. We note that all C_i are subgraph of their partner L_i , formed by merging all orbit vertices corresponding to isomorphic graph states. This can be seen by observing that isomorphic graph states have isomorphic neighbourhoods in L_i .

We find there are typically more than one C_i orbit (for fixed i), as most C_i orbits do not contain every isomorphism of its member graph states (e.g. Fig. 1d)—the entanglement possessed is distributed in different ways between the parties. For example, there are three equivalent orbits of L_4 (one of which is shown in Fig. 1), each containing different isomorphisms of their component graph states. Some entanglement classes have only one orbit, which contains every isomorphism of the graph states. For example, the classes which contain the ‘star’ and fully-connected graph states. These orbits are composed of $|L_i| = n + 1$ graph states (vertices) and are themselves a ‘star’ graph (e.g. Fig. 1b).

As in L_i orbits, edges of a C_i orbit are undirected. However, as a guide to the eye we display directed edges for C_i orbits when those edges are labelled, as this allows the reader to identify which of the displayed graph state vertices are locally complemented to reach the output graph (see Fig. 1c,e,f).

2.3 Orbit exploration

Mapping the orbit of the i^{th} entanglement class, M_i containing a graph state $|G\rangle$, is a graph exploration problem. Here, we use an exhaustive breadth-first exploration to traverse the entire orbit, cataloguing each graph state (vertices of the orbit) along with how local complementation links them (edges of the orbit). We start with a single graph state G , taken from ref. 17, in our catalogue, and perform each possible local complementation on it. In doing so, we discover up to n new orbit vertices and up to n new orbit edges. Then we perform every possible local complementation on those output graph states and catalogue the outputs by comparing them to graph states which we have already found. This is repeated until every local complementation has been performed on every graph state in the catalogue (and no new graph states or edges are found).

To map an n -qubit orbit, M_i , which contains $|M_i|$ graph states requires $O(n|M_i|)$ local complementations and graph comparisons. By ‘graph comparison’, we mean evaluating if two graphs are equal, or calling GRAPHISOMORPHISM (depending on whether $M_i = L_i$ or $M_i = C_i$ respectively). Linear savings can be made by noting that local complementation is self inverse, and has no effect when applied to a vertex of

Class	$ Q $	$ e $	E_S	rwd	$ C_i $	$ E_i $	$ E_i / C_i $	χ_g	χ_{C_i}	χ_g^e	Tree	\bar{d}_i	$\max(d_i)$	$ \text{aut} $	2D	Loop	E.	H.
3	4	3	1	1	2	2	1	2	2	3	✓	1	1	1	✓	✓	✗	✗
4	4	3	2	1	4	5	1.25	2	2	2	✓	1.67	3	1	✓	✓	✗	✗
5	5	4	1	1	2	2	1	2	2	4	✓	1	1	1	✓	✓	✗	✗
6	5	4	2	1	6	9	1.5	2	2	3	✗	1.8	3	2	✓	✓	✓	✓
7	5	4	2	1	10	19	1.9	2	3	2	✗	2.04	3	1	✓	✓	✗	✓
8	5	5	$2 < 3$	2	3	3	1	3	2	3	✓	1.33	2	1	✓	✓	✗	✗
9	6	5	1	1	2	2	1	2	2	5	✓	1	1	1	✓	✓	✗	✗
10	6	5	2	1	6	9	1.5	2	2	4	✗	1.8	3	2	✓	✓	✓	✓
11	6	5	2	1	4	5	1.25	2	2	3	✓	1.67	3	1	✓	✓	✗	✗
12	6	5	2	1	16	34	2.13	2	3	3	✗	2.25	3	3	✗	✓	✗	✓
13	6	5	3	1	10	20	2	2	3	3	✗	2.04	3	1	✓	✓	✗	✓
14	6	5	3	1	25	58	2.32	2	3	2	✗	2.51	5	2	✗	✓	✓	✗
15	6	6	2	1	5	8	1.6	2	3	3	✗	1.7	3	1	✓	✓	✗	✗
16	6	6	3	1	5	9	1.8	3	3	3	✗	1.7	3	1	✓	✓	✗	✗
17	6	6	3	2	21	47	2.24	3	3	3	✗	2.32	4	0	✗	✓	✗	✓
18	6	6	3	2	16	29	1.81	2	3	2	✗	2.22	4	0	✗	✓	✗	✗
19	6	9	$3 < 4$	2	2	2	1	3	2	3	✓	1	1	1	✓	✓	✗	✗
20	7	6	1	1	2	2	1	2	2	6	✓	1	1	1	✓	✓	✗	✗
21	7	6	2	1	6	9	1.5	2	2	5	✗	1.8	3	2	✓	✓	✓	✓
22	7	6	2	1	6	9	1.5	2	2	4	✗	1.8	3	2	✓	✓	✓	✓
23	7	6	2	1	16	34	2.13	2	3	4	✗	2.25	3	3	✗	✓	✗	✓
24	7	6	2	1	10	19	1.9	2	3	3	✗	2.04	3	1	✓	✓	✗	✓
25	7	6	3	1	10	20	2	2	3	4	✗	2.04	3	1	✓	✓	✗	✓
26	7	6	3	1	16	35	2.19	2	3	3	✗	2.25	3	3	✗	✓	✗	✓
27	7	6	3	1	44	114	2.59	2	3	3	✗	2.84	5	3	✗	✓	✓	✓
28	7	6	3	1	44	118	2.68	2	3	3	✗	2.84	5	3	✗	✓	✓	✓
29	7	6	3	1	14	30	2.14	2	3	3	✗	2.34	5	1	✓	✓	✗	✓
30	7	6	3	1	66	191	2.89	2	3	2	✗	3.05	6	2	✗	✓	✗	✓
31	7	7	2	1	10	20	2	2	3	4	✗	2.04	3	1	✓	✓	✗	✓
32	7	7	3	1	10	21	2.1	3	3	4	✗	2.04	3	1	✓	✓	✗	✓
33	7	7	3	2	21	47	2.24	3	3	4	✗	2.31	4	0	✗	✓	✗	✓
34	7	7	3	1	26	68	2.62	2	3	3	✗	2.50	4	3	✗	✓	✗	✓
35	7	7	3	2	36	98	2.72	3	3	3	✗	2.54	4	1	✗	✓	✗	✓
36	7	7	3	1	28	70	2.5	3	3	3	✗	2.62	5	3	✗	✓	✗	✓
37	7	7	3	2	72	206	2.86	3	3	3	✗	3.06	5	2	✗	✓	✗	✓
38	7	7	3	2	114	336	2.94	2	3	3	✗	3.29	6	2	✗	✓	✓	✓
39	7	7	$3 < 4$	2	56	157	2.80	3	4	3	✗	2.85	5	1	✗	✓	✗	✓
40	7	7	$3 < 4$	2	92	271	2.95	3	3	3	✗	3.02	7	1	✗	✗	✗	✗
41	7	8	$3 < 4$	2	57	164	2.88	3	3	3	✗	2.79	5	1	✗	✓	✗	✓
42	7	8	$3 < 4$	2	33	80	2.42	3	5	3	✗	2.43	5	0	✗	✓	✗	✓
43	7	9	3	2	9	16	1.78	2	3	3	✗	1.81	3	1	✓	✓	✗	✗
44	7	9	$3 < 4$	2	46	109	2.37	3	5	3	✗	2.81	5	0	✗	✓	✗	✓
45	7	10	$3 < 4$	2	9	16	1.78	3	3	4	✗	1.97	4	0	✓	✓	✗	✗

Table 1: A selection of properties of C_i (see Appendix Figure 11 for a table showing a representative graph state from each class of $n < 9$ qubits). Here, $|Q|$ is the number of qubits of the orbit's graph states, $|e|$ is smallest number of edges of any graph state member of C_i . The class's Schmidt measure, E_S , is written $a < b$ to compactly express lower (a) and upper (b) bounds, when an exact value is not known¹¹. rwd is the class's rank width, $|C_i|$ is the size of the orbit, $|E_i|$ is the number of edges on the orbit, χ_g is the minimum chromatic number of the graph states in the class, χ_{C_i} is the orbit's chromatic number, χ_g^e is the minimum chromatic index of the graph states in the class (which corresponds to the minimum number of CZ gates required to prepare them), d_i are the distances between vertices on the orbit ($\max(d_i)$ is therefore the diameter of the orbit), ‘Tree’ is whether the orbit is a tree (excluding self-loops), ‘2D’ is whether the orbit is planar, ‘Loop’ is whether the orbit has any self-loops, ‘E.’ (‘H.’) is whether the graph has a cycle in which each edge (vertex) of the orbit is visited precisely once. We note the correlation of orbit diameter, and orbit chromatic index with the Schmidt measure and rank width of the entangled state. Properties of L_i orbits may differ to their C_i equivalent.

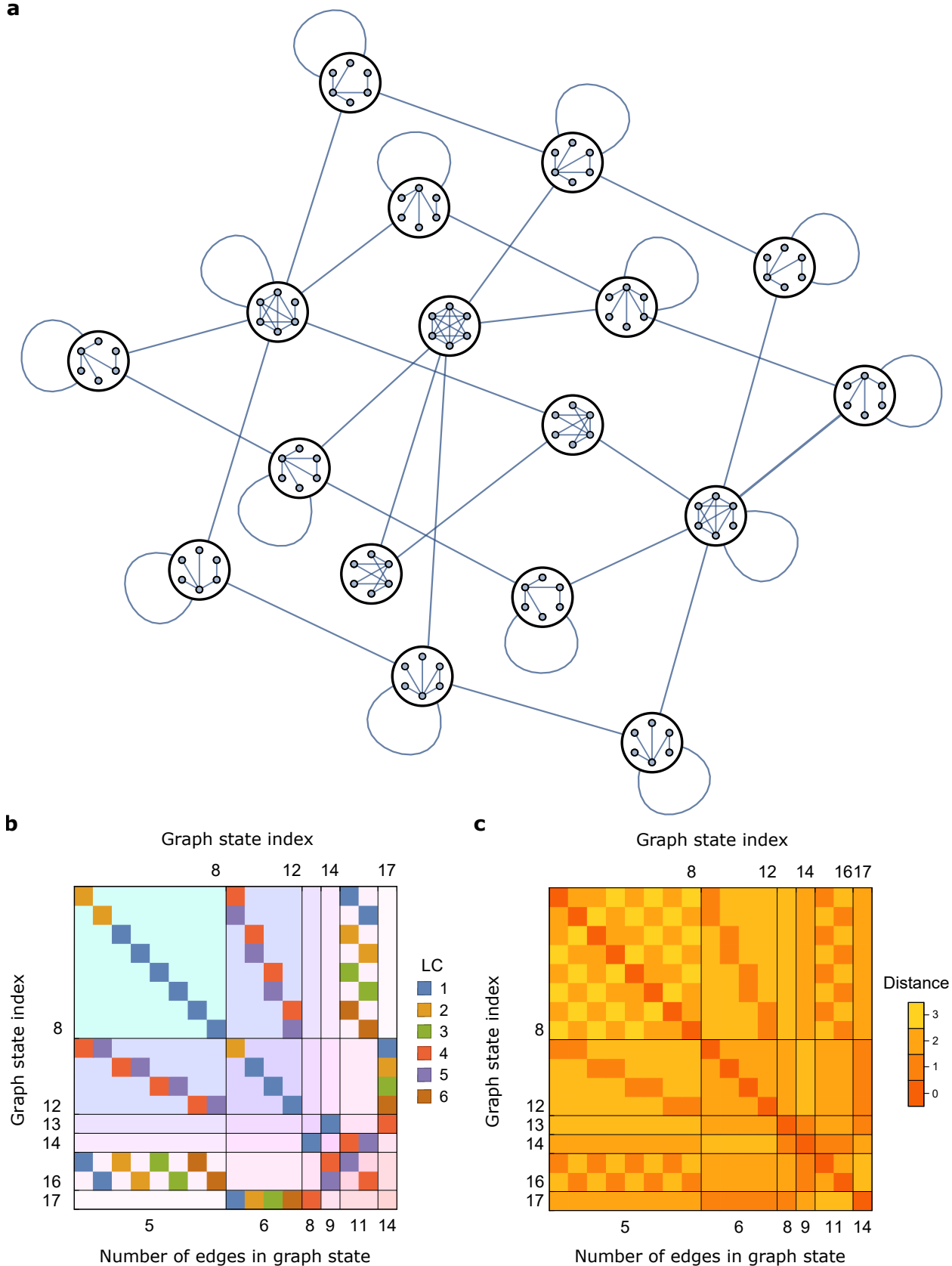


Fig. 2: Local complementation orbit L_{10} . **a.** The orbit L_{10} . **b.** The adjacency matrix of L_{10} . **c.** The distance matrix of L_{10} . The adjacency matrix of a graph, A , has a row and column for each of the graph's vertices. For each edge (i, j) present in graph we write $A_{ij} = n$, where n is the lowest index of a local complementation that links them. Otherwise $A_{ij} = 0$. Similarly, the distance matrix, D , gives the distance between two vertices: D_{ij} is equal to the minimum number of edges that must be traversed to get from vertex i to vertex j .

degree 1.

We use this method to explore the L_i for $n \leq 8$ and C_i for $n \leq 9$, that is, up to graph state entanglement class $i = 146$ and $i = 586$ respectively. The largest of these orbits contains 3248 and 8836 graph states, respectively. GRAPHISOMORPHISM is a costly routine, belonging to the complexity class NP. Exploration of C_i makes heavy use of GRAPHISOMORPHISM, calling it up to $n|C_i|$ times. However, since $|C_i| \ll |L_i|$, and our graph states are of modest size, exploring C_i up to 9 qubits required less computational time than exploring L_i up to 8 qubits.

When exploring C_i orbits, we notice that local complementing symmetric vertices of an input graph state will result in the same output graph state. For example, in Fig. 1c, local complementing any of the vertices of the fully connected graph state will result in the same output, while for the adjacent ‘star’ tree graph state, there are two inequivalent local complementation operations—the centre and the leaves.

The sets of vertices which result in isomorphic graphs under local complementation can be found by computing the automorphism group of each graph state—vertices that are exchanged in an automorphism result in isomorphic graphs. Hence, by computing the automorphism group of each graph state as it is discovered, and only local complementing the reduced subset of graph state vertices that are not equivalent, a saving can be made. Here, only $\tilde{n}|C_i|$ comparisons (and hence calls to GRAPHISOMORPHISM) need be made (where $\tilde{n} = |E_i|/|C_i|$ is the mean number of non-symmetric vertices on the graph states of C_i). In practice, the AUTOMORPHISMGROUP is computed in order to solve GRAPHISOMORPHISM²⁶. Hence a linear speedup is achieved. By examining our set of computed orbits, we find this technique reduces the number of calls to GRAPHISOMORPHISM by at least half for $n \leq 9$.

3 Results

We compute a variety of graph properties of C_i orbits of 3-7 qubits and display them in Table 1. For example we display the Schmidt measure, E_S , which is known to be a useful entanglement monotone for graph states^{11,27}. We also compute the graph state’s rank width, $\text{rwd}(G)$ ^{14,28}. We also compute parameters of the orbit such as the chromatic number, chromatic index, the mean and maximum distances (diameter), and the size of the orbits automorphism group.

As per the canonical indexing of graph state entanglement classes, we list the minimum degree of each orbit: the smallest number of edges of any of the orbit’s graph states. This corresponds to the minimum number of CZ gates required to generate that entanglement class. We also provide the graph state’s minimum chromatic index (minimal edge colouring number), which corresponds to the minimum number of time steps required to generate a state in that entanglement class¹⁷ (assuming CZs can be performed between each qubit arbitrarily).

We find correlations between orbit parameters and compute their Pearson correlation coefficients, $-1 < r(x, y) < 1$, for orbit parameters x, y . For example, the graph state Schmidt measure, E_S correlates with orbit diameter with $r(\max(d_i), E_S) = \{0.77 \pm 0.02, 0.93 \pm 0.02\}$, for C_i and L_i orbits respectively. Here, if the Schmidt measure is not known,

we take the average value of the bounds, which are rarely loose. Orbit chromatic number and Schmidt measure have correlation coefficients of $r(\chi_{C_i}, E_S) = \{0.67 \pm 0.02, 0.70 \pm 0.45\}$, while orbit chromatic index and Schmidt measure correlate with $r(\chi_{C_i}^e, E_S) = \{0.81 \pm 0.04, 0.82 \pm 0.06\}$ for $n \leq 8$ and $n \leq 7$ respectively. Meanwhile, orbit chromatic number does not correlate with minimum graph state chromatic index, $r(\chi_{C_i}, \chi_g^e) = \{0.032 \pm 0.04, -0.09 \pm 0.09\}$. We note that Schmidt measure correlates with rank width and minimum edge count with $r(E_S, \text{rwd}) = 0.62 \pm 0.03$ and $r(E_S, |e|) = 0.78 \pm 0.02$, but not with graph state chromatic index $r(E_S, \chi_g^e) = -0.17 \pm 0.0$. Interestingly, Schmidt rank (and therefore orbit chromatic index), strongly correlates with minimum edge count (the total number of CZs required to prepare an entanglement class) but not with graph state chromatic index (the number of CZ time steps required to prepare an entanglement class). Lattice graph states, which contain states universal for quantum computation, have constant CZ time steps preparation complexity, however their rank width must grow faster than logarithmically²¹.

Some properties of an entanglement class’ graph states can be deduced from properties of their orbit. For example, class no. 40 has no self-loops. This implies that none of its member graph states have a vertex of degree 1. This is the only orbit with this property up to $n = 7$, but 9% of L_i orbits up to $n = 9$ have it.

We also observe that local complementations commute when the neighbourhoods of the two indices are disjoint. This creates a cycle in the graph state’s orbit. Hence it can be deduced that orbits which are trees only contain graph states in which all vertices whose local complementation results in different states share parts of their neighbourhoods. We note that only GreenbergerHorneZeilinger (GHZ) entanglement gives rise to L_i orbits that are trees (for $n \leq 8$), and these contain only two graph states. Meanwhile there is one three-vertex orbit and three four-vertex C_i orbits which are trees. These are connected in a line with one and two self-loops respectively (see Fig. 1e).

Interestingly, some C_i orbits are isomorphic (see Figs. 1c, f and 3). A simple example is that of GHZ entanglement of n qubits. This class always contains only the n -qubit ‘star’ and fully connected graph states. Hence the C_i orbits of GHZ entanglement are always the two qubit connected graph—analogous states give rise to analogous orbits across qubit numbers (see Fig. 3b). In contrast, no L_i orbits are isomorphic for $n \leq 8$.

The proportion of all graphs which are asymmetric tends towards zero as the number of vertices tends towards infinity²⁹, ($\sim 50\%$ of unlabelled 9-vertex graphs) However, the majority of the orbits we compute are symmetric (75% of 9-qubit orbits have a non-empty automorphism group), including orbits containing thousands of graph states. The relationship between an orbit’s symmetry and the graph state symmetries of its component graph states left for future work.

Many of the computed parameters, such as Schmidt measure, rank width and automorphism group are exponentially difficult problems. The rank width, while exponential in nature, can be computed exactly³⁰, while the Schmidt measure requires a nonconvex, nonlinear optimisation, and so is more challenging. We rely on previously computed¹⁷ bounds of

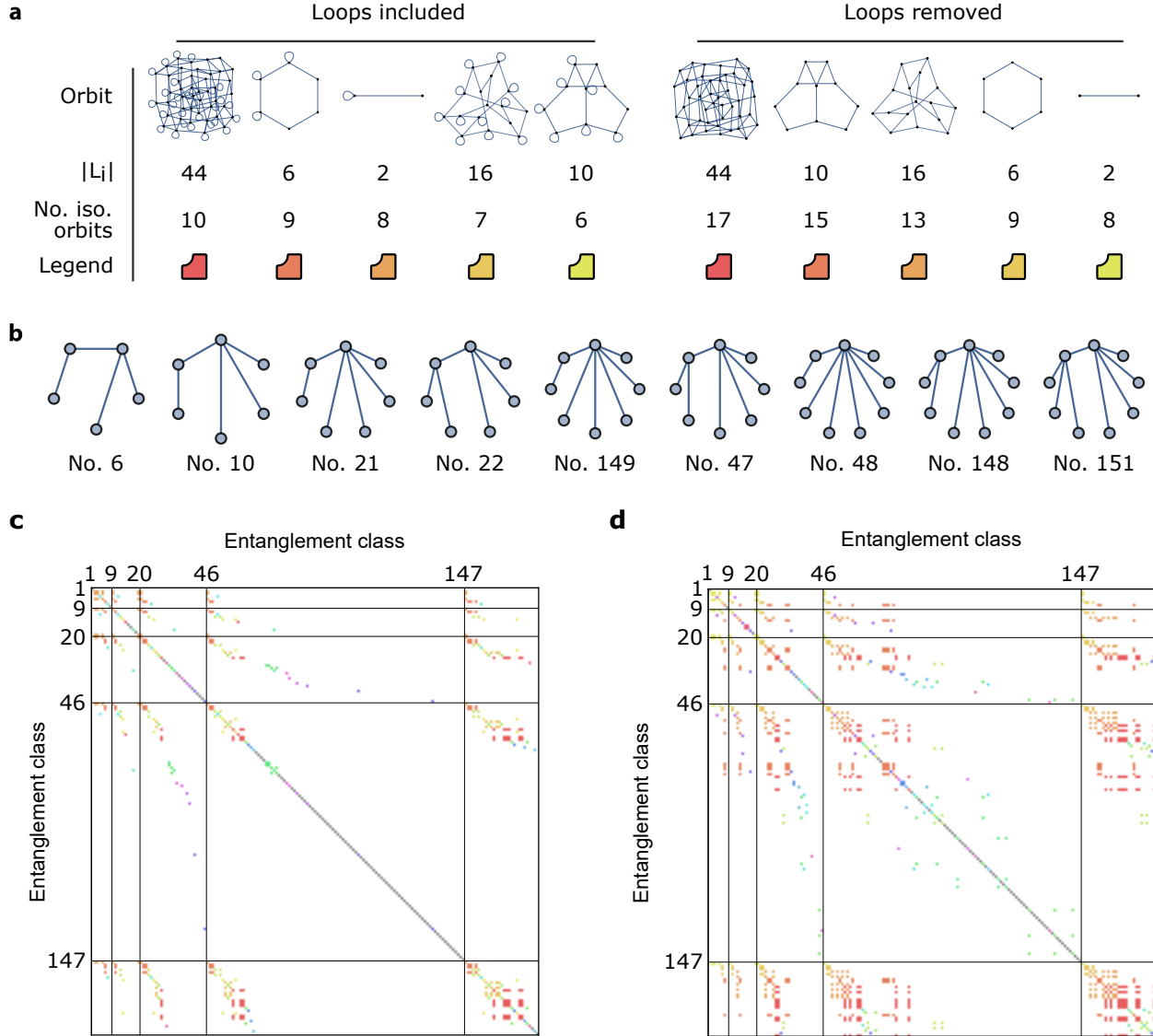


Fig. 3: Isomorphism of local complementation orbits. **a.** The five most common orbits up to class 150, considering orbit self-loops and not. **b.** Canonical, minimum-edge representatives of the orbits C_i for $i = 6, 10, 21, 22, 47, 48, 148, 149, 151$, each of which are isomorphic to one another (an order-six ring with three adjacent self-loops, see a). **c.** Isomorphism of orbits C_i . $I_{ij} = 1$ if orbit C_i and C_j are isomorphic. Entries are coloured by isomorphism. Regions of equal qubit number are demarcated. **d.** Isomorphism of C_i orbits with self-loops removed.

the Schmidt measure, while computing the rank width using the software ‘SAGE’. Though our graph states are small, there is an exponential number of entanglement classes as qubit number is increased. Further, many of the graph metrics discussed, such as colourability belong to complexity class NP. As such, they become challenging to compute on dense orbits with thousands of vertices. For this reason we computed the chromatic index only for $n \leq 8$ and $n \leq 7$ for C_i and L_i orbits respectively. All graph colouring computations were performed with the software ‘IGraph/M’.

Due to their connectivity and scale, the majority of orbits we explored are far too complex to view directly, as we did in Fig. 1. We can instead represent them with matrices. Fig. 2 shows the adjacency matrices and distance matrices of class L_{10} . We order the matrix by isomorphism, edge count, and then lexicographically by their lexicographically sorted edgelists. Further, we demarcate regions of the plot

which correspond to graph states that have the same number of edges and that are isomorphic to one another for C_i and L_i respectively. In both cases, the adjacency matrices show structure related to these regions.

There is variety and scale in the 587 C_i orbits and 147 L_i orbits we have computed which cannot be reproduced in a single article. A curated selection of orbits is displayed in Appendix Section 1, and the full data available online.

4 Discussion

It is likely that future quantum information processors will have restricted two-qubit gate topology, due to the qubit’s physical locations and proximity. Since single-qubit operations are commonly faster or higher-fidelity than two-qubit gates, local complementation may be used to improve a device’s speed or fidelity²³. For a prescriptive method, the relationship between orbits and nonlocal CZ gates must be

known. A complete map of this type would describe how all n -qubit graph states are related to one another, and provide a look up table for optimal transformations between them. From here, the addition of vertex deletion would give a complete map of graph states under LC+LPM+CC operations (the vertex minor problem). A doubly-exponential problem, computation of these maps appears to be infeasible for even modest n . For small graphs, however, such a map may be enlightening—the exploration is left for future work.

Knowledge of the orbits of local complementation may also enable in quantum secret sharing and quantum networks^{7,31}. A graph state may be distributed between separated parties, each of whom can perform local operations and communicate with their neighbours (according to the graph state structure). This allows different quantum protocols to be implemented using a resource which has already been distributed spatially. If the parties only have knowledge of their own neighbourhood, and each party performs local complementation at random, the shared state can be scrambled. Numerically, we find the stationary distributions generated by random walks on the orbits appear to tend towards uniform as orbit size increases, implying this ‘scrambling’ is effective. This could be formalised further by investigating mixing rates.

Local complementation allows the entanglement of a resource state to be utilised differently^{31–33}. That is, a resource state can be transformed into any other state from its entanglement class, and used according to its shape. Though this is equivalent to changing the protocol measurement bases, considering locally equivalent graph states as a new state preserves the standard language of measurement-based protocols (measurement in the X - Y plane and Z directions). Generally, local complementation has merit in applications where qubits are in inequivalent spatial locations—it illustrates the many functions of a given entanglement.

In some quantum computer architectures, such as those for linear optical quantum computing³⁴, percolated resource states are generated probabilistically. These states have a randomly generated structure, and hence some are more powerful than others, for example they may have more favourable connectivity for pathfinding³⁵ or loss tolerance^{36,37}, which may be optimised by local complementation. Though the entanglement class of any useful resource state will be too large to compute directly, it may be possible to develop heuristics for using local complementation to optimise local regions of the (locally connected) resource. These heuristics may be explored and verified with the algorithm of ref. 19.

Our library of orbits, available online²⁴, comprises 35 MB compressed. All computations thus far were performed using a single core of an Intel i5 CPU in Mathematica. Exploration up to $n = 12$, where representative graph states of each orbit are known, is feasible if a compiled language and parallelism are employed. Extending the database further is a significant computational challenge, as, though an exact scaling is not known, the number of graph state entanglement classes grows super-exponentially for $n \leq 12$ qubits.

Our exploration opens some novel lines of questioning. For example, what is the relationship between graph state properties, such as Schmidt measure, and orbit properties, such as colourability? Is it possible to completely map

LC+LPM+CC operations up to 12 qubits? What new applications are possible utilising knowledge of LC orbits?

Stabiliser state entanglement is—and will continue to be—at the core of quantum information protocols. The resource we provide gives a new handle to investigate the rich relationship between graph theory, stabiliser state entanglement, and applications of quantum information.

References

- [1] Raussendorf, R. Measurement-based quantum computation with cluster states. *International Journal of Quantum Information* **7**, 1053–1203 (2009).
- [2] Veldhorst, M., Eenink, H., Yang, C. & Dzurak, A. Silicon cmos architecture for a spin-based quantum computer. *Nature Communications* **8**, 1766 (2017).
- [3] Lekitsch, B. *et al.* Blueprint for a microwave trapped ion quantum computer. *Science Advances* **3**, e1601540 (2017).
- [4] Alexander, R. N. *et al.* One-way quantum computing with arbitrarily large time-frequency continuous-variable cluster states from a single optical parametric oscillator. *Physical Review A* **94**, 032327 (2016).
- [5] Asavanant, W. *et al.* Time-domain multiplexed 2-dimensional cluster state: Universal quantum computing platform. *arXiv preprint arXiv:1903.03918* (2019).
- [6] Barends, R. *et al.* Superconducting quantum circuits at the surface code threshold for fault tolerance. *Nature* **508**, 500 (2014).
- [7] Markham, D. & Sanders, B. C. Graph states for quantum secret sharing. *Physical Review A* **78**, 042309 (2008).
- [8] Ji, Z., Chen, J., Wei, Z. & Ying, M. The lu-lc conjecture is false. *arXiv preprint arXiv:0709.1266* (2007).
- [9] Cabello, A., López-Tarrida, A. J., Moreno, P. & Portillo, J. R. Entanglement in eight-qubit graph states. *Physics Letters A* **373**, 2219–2225 (2009).
- [10] Anders, S. & Briegel, H. J. Fast simulation of stabilizer circuits using a graph-state representation. *Physical Review A* **73**, 022334 (2006).
- [11] Hein, M., Eisert, J. & Briegel, H. J. Multiparty entanglement in graph states. *Physical Review A* **69**, 062311 (2004).
- [12] Van den Nest, M., Dehaene, J. & De Moor, B. Graphical description of the action of local clifford transformations on graph states. *Physical Review A* **69**, 022316 (2004).
- [13] Hein, M. *et al.* Entanglement in graph states and its applications. *arXiv preprint quant-ph/0602096* (2006).
- [14] Dahlberg, A. & Wehner, S. Transforming graph states using single-qubit operations. *Phil. Trans. R. Soc. A* **376**, 20170325 (2018).

[15] Dahlberg, A., Helsen, J. & Wehner, S. The complexity of the vertex-minor problem. *arXiv preprint arXiv:1906.05689* (2019).

[16] Danielsen, L. E. & Parker, M. G. On the classification of all self-dual additive codes over $gf(4)$ of length up to 12. *Journal of Combinatorial Theory, Series A* **113**, 1351–1367 (2006).

[17] Cabello, A., Danielsen, L. E., Lopez-Tarrida, A. J. & Portillo, J. R. Optimal preparation of graph states. *Physical Review A* **83**, 042314 (2011).

[18] Bouchet, A. An efficient algorithm to recognize locally equivalent graphs. *Combinatorica* **11**, 315–329 (1991).

[19] Van den Nest, M., Dehaene, J. & De Moor, B. Efficient algorithm to recognize the local clifford equivalence of graph states. *Physical Review A* **70**, 034302 (2004).

[20] Dahlberg, A., Helsen, J. & Wehner, S. How to transform graph states using single-qubit operations: computational complexity and algorithms. *arXiv preprint arXiv:1805.05306* (2018).

[21] Van den Nest, M., Dür, W., Vidal, G. & Briegel, H. Classical simulation versus universality in measurement-based quantum computation. *Physical Review A* **75**, 012337 (2007).

[22] Dahlberg, A., Helsen, J. & Wehner, S. Counting single-qubit clifford equivalent graph states is $\#P$ -complete. *arXiv preprint arXiv:1907.08024* (2019).

[23] Adcock, J. C., Morley-Short, S., Silverstone, J. W. & Thompson, M. G. Hard limits on the postselectability of optical graph states. *Quantum Science and Technology* **4**, 015010 (2019).

[24] Mapping graph states under local complementation <https://github.com/ja0877/graphorbits>.

[25] Rokicki, T., Kociemba, H., Davidson, M. & Dethridge, J. The diameter of the Rubik’s cube group is twenty. *SIAM Review* **56**, 645–670 (2014).

[26] McKay, B. D. & Piperno, A. Practical graph isomorphism II. *Journal of Symbolic Computation* **60**, 94–112 (2014).

[27] Eisert, J. & Briegel, H. J. Schmidt measure as a tool for quantifying multiparticle entanglement. *Physical Review A* **64**, 022306 (2001).

[28] Van den Nest, M., Miyake, A., Dür, W. & Briegel, H. J. Universal resources for measurement-based quantum computation. *Physical Review Letters* **97**, 150504 (2006).

[29] Erdős, P. & Rényi, A. Asymmetric graphs. *Acta Mathematica Hungarica* **14**, 295–315 (1963).

[30] Oum, S.-I. Computing rank-width exactly. *Information Processing Letters* **109**, 745–748 (2009).

[31] Hahn, F., Pappa, A. & Eisert, J. Quantum network routing and local complementation. *NPJ Quantum Information* **5**, 1, 5–7 (2019).

[32] Joo, J. & Feder, D. L. Edge local complementation for logical cluster states. *New Journal of Physics* **13**, 063025 (2011).

[33] Zwerger, M., Dür, W. & Briegel, H. Measurement-based quantum repeaters. *Physical Review A* **85**, 062326 (2012).

[34] Gimeno-Segovia, M., Shadbolt, P., Browne, D. E. & Rudolph, T. From three-photon Greenberger-Horne-Zeilinger states to ballistic universal quantum computation. *Physical Review Letters* **115**, 020502 (2015).

[35] Morley-Short, S. et al. Physical-depth architectural requirements for generating universal photonic cluster states. *Quantum Science and Technology* **3**, 015005 (2017).

[36] Rudolph, T. Why I am optimistic about the silicon-photonic route to quantum computing. *APL Photonics* **2**, 030901 (2017).

[37] Morley-Short, S., Gimeno-Segovia, M., Rudolph, T. & Cable, H. Loss-tolerant teleportation on large stabilizer states. *Quantum Science and Technology* (2018).

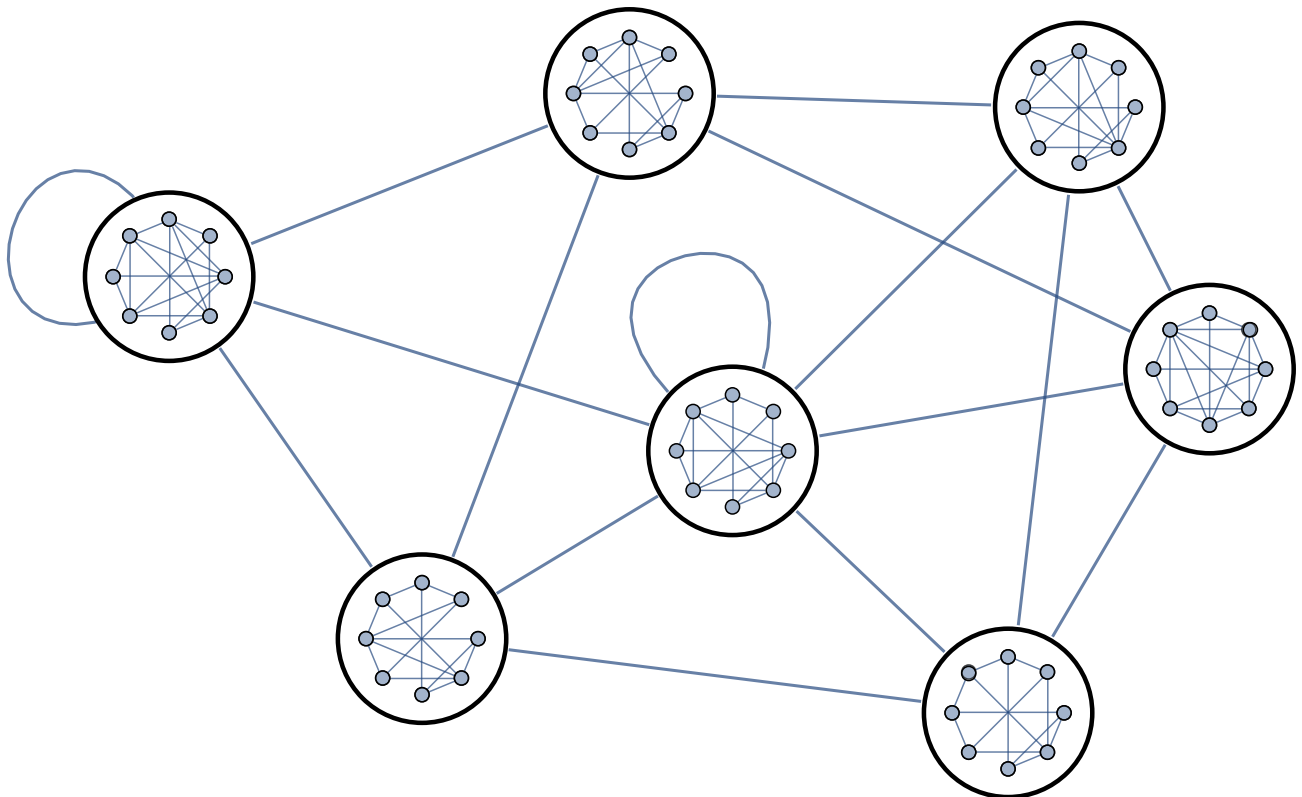
Acknowledgements

We would like to thank Caterina Vigliar, Sam Pallister, Will McCutcheon, and John G. Rarity for their invaluable help. The computer programs ‘IGraph/M’ and ‘SAGE’ were vital for evaluating difficult to compute properties of our extensive library of graphs. This work was supported by EPSRC Programme Grant EP/L024020/1, the EPSRC Quantum Engineering Centre for Doctoral Training EP/L015730/1, and the ERC Starting Grant ERC-2014-STG 640079. JWS acknowledges the generous support of the Leverhulme Trust, through Leverhulme Early Career Fellowship ECF-2018-276.

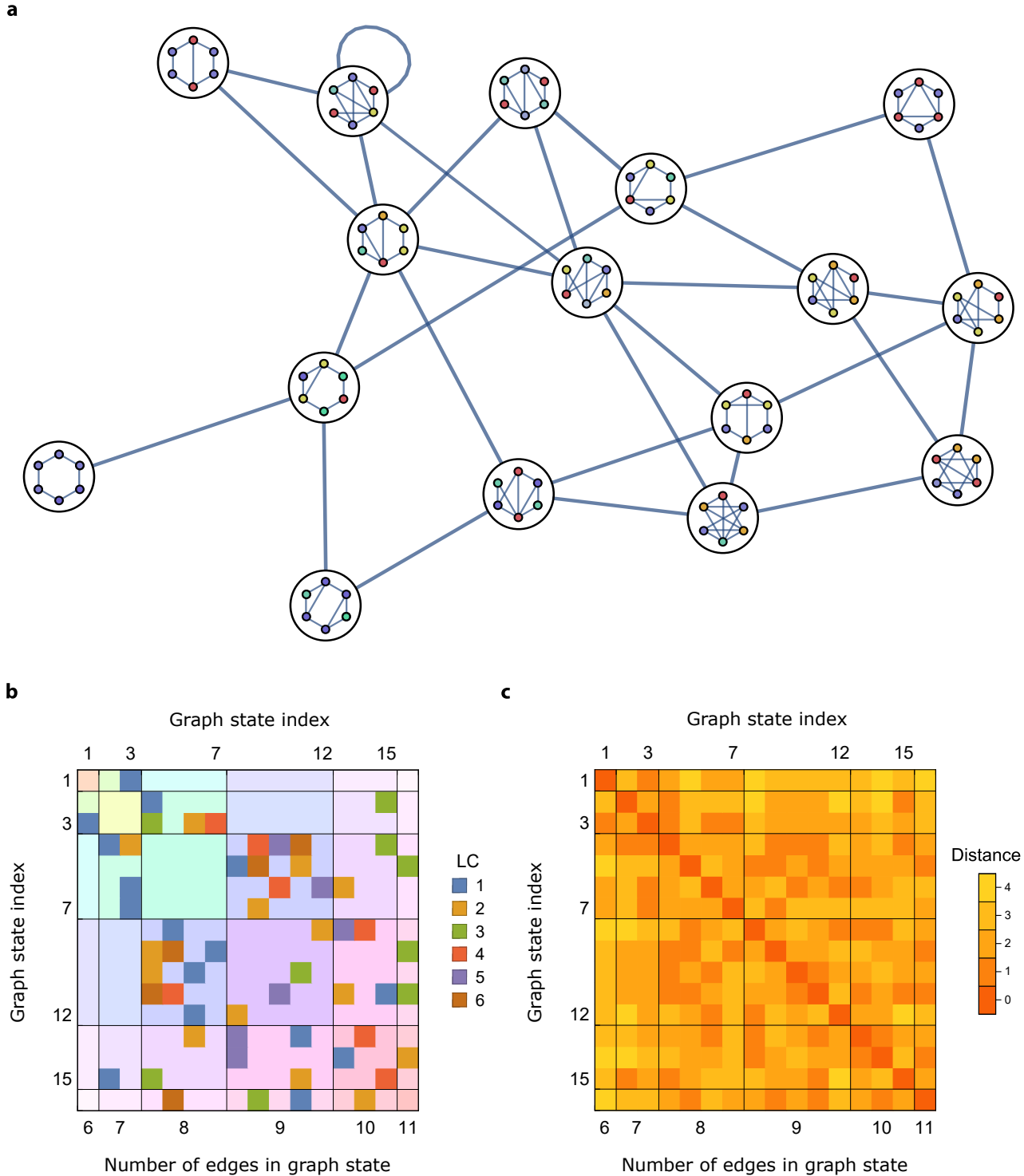
Appendix

1 A gallery of graph state orbits

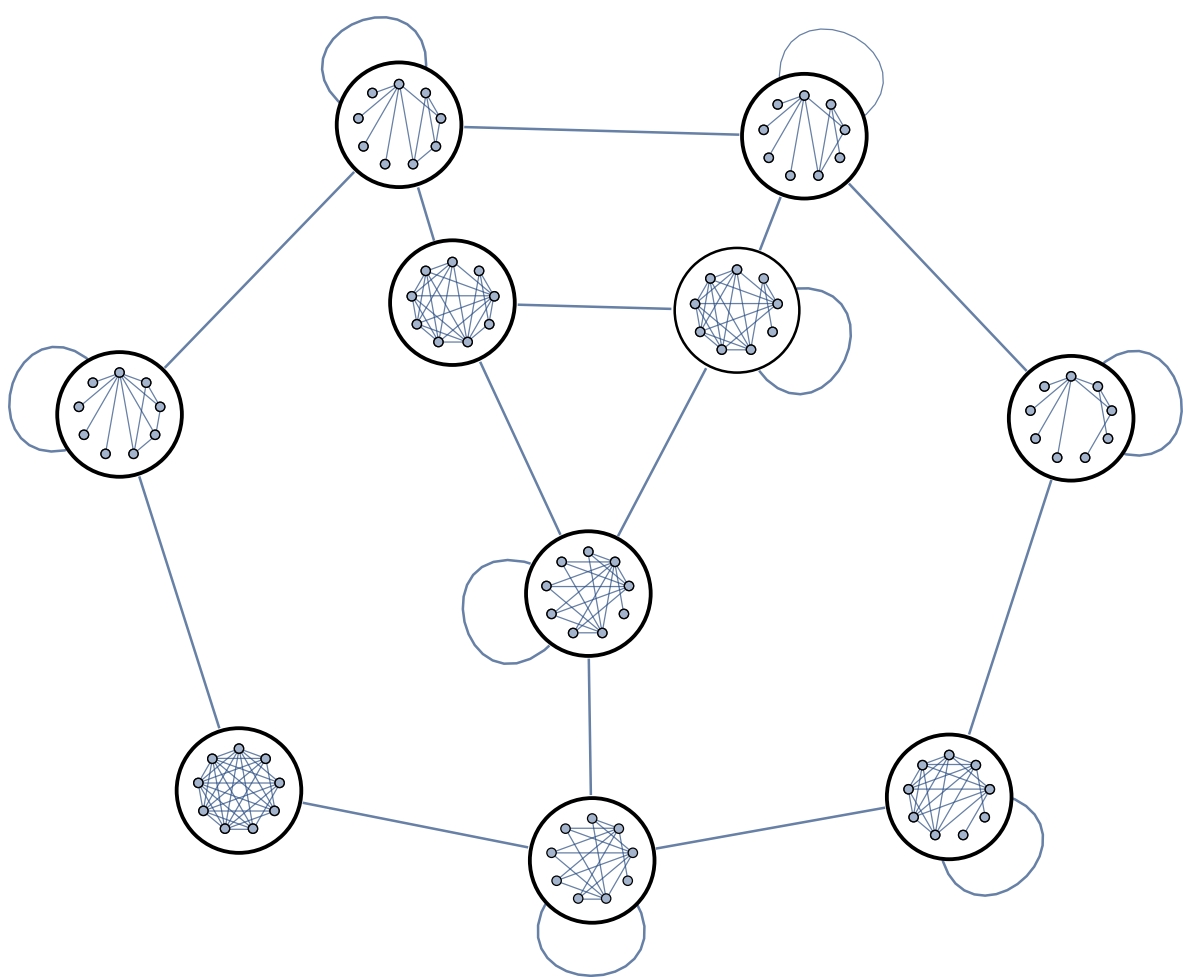
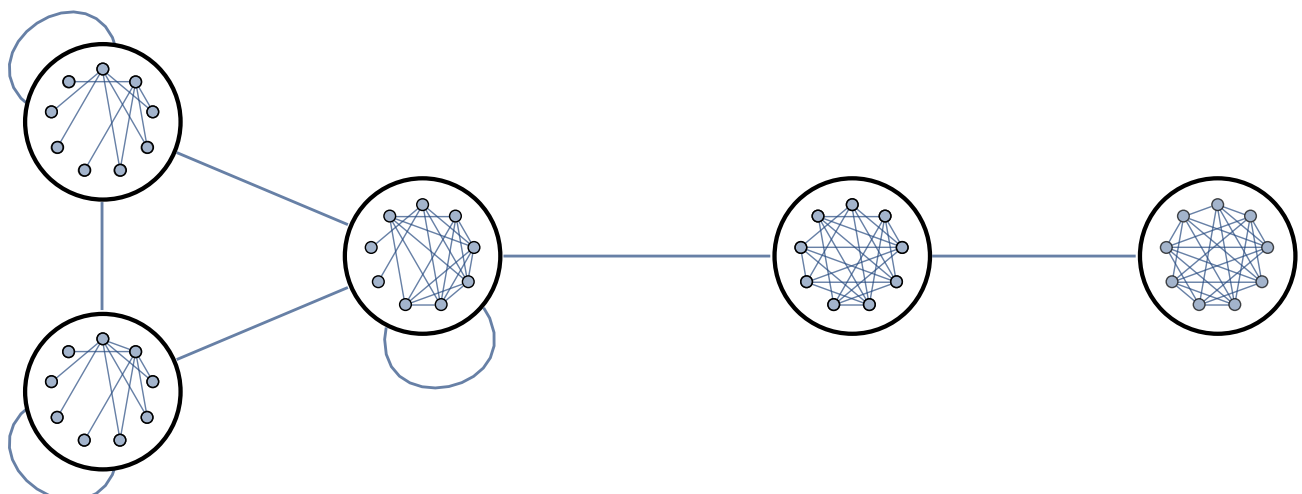
We map over 600 orbits, most of which are vastly too large and complex to display. In this Appendix, we exhibit a curated selection of orbits to demonstrate the variety of form they display.

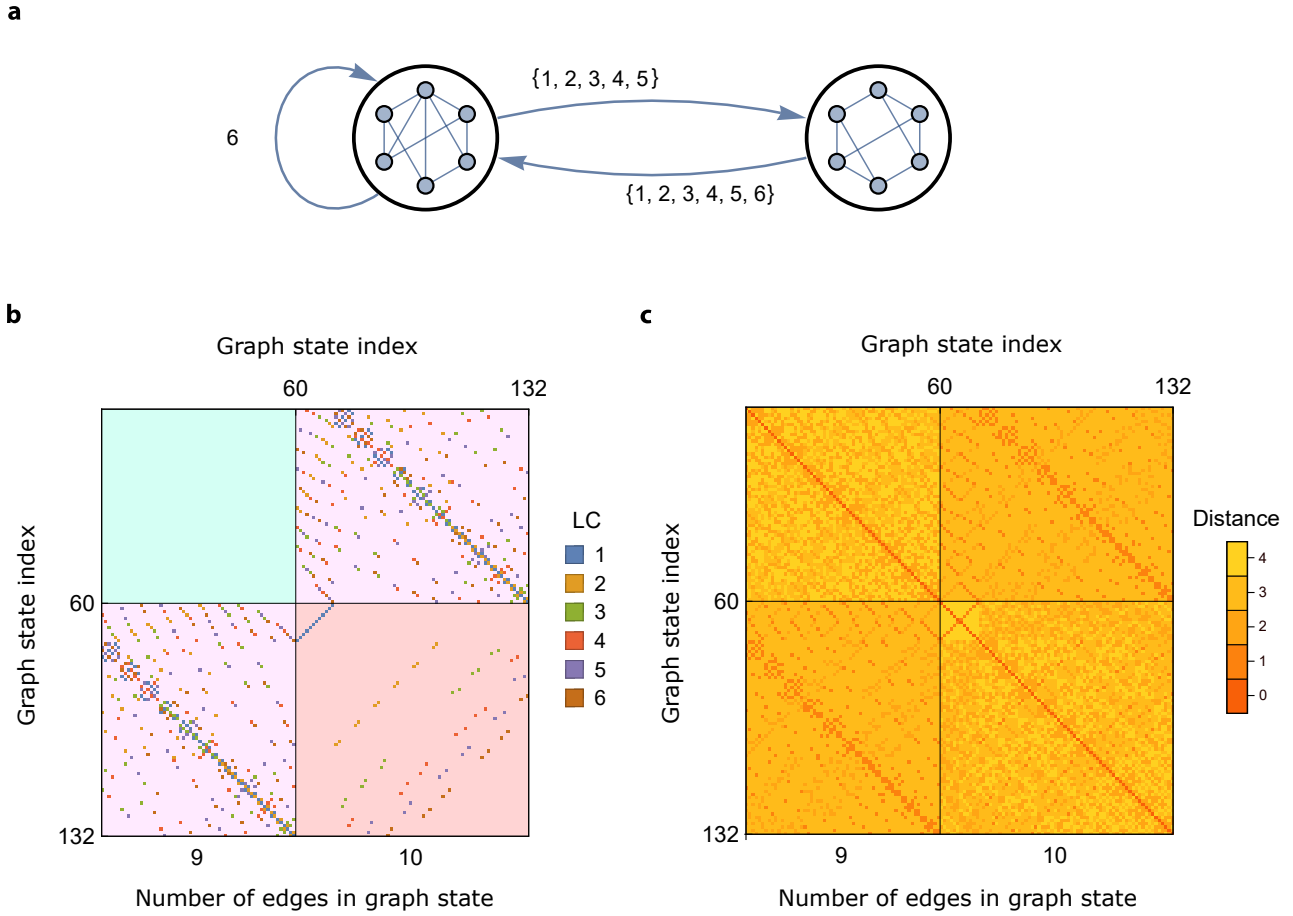


Appendix Figure 1: Orbit C_{145} .

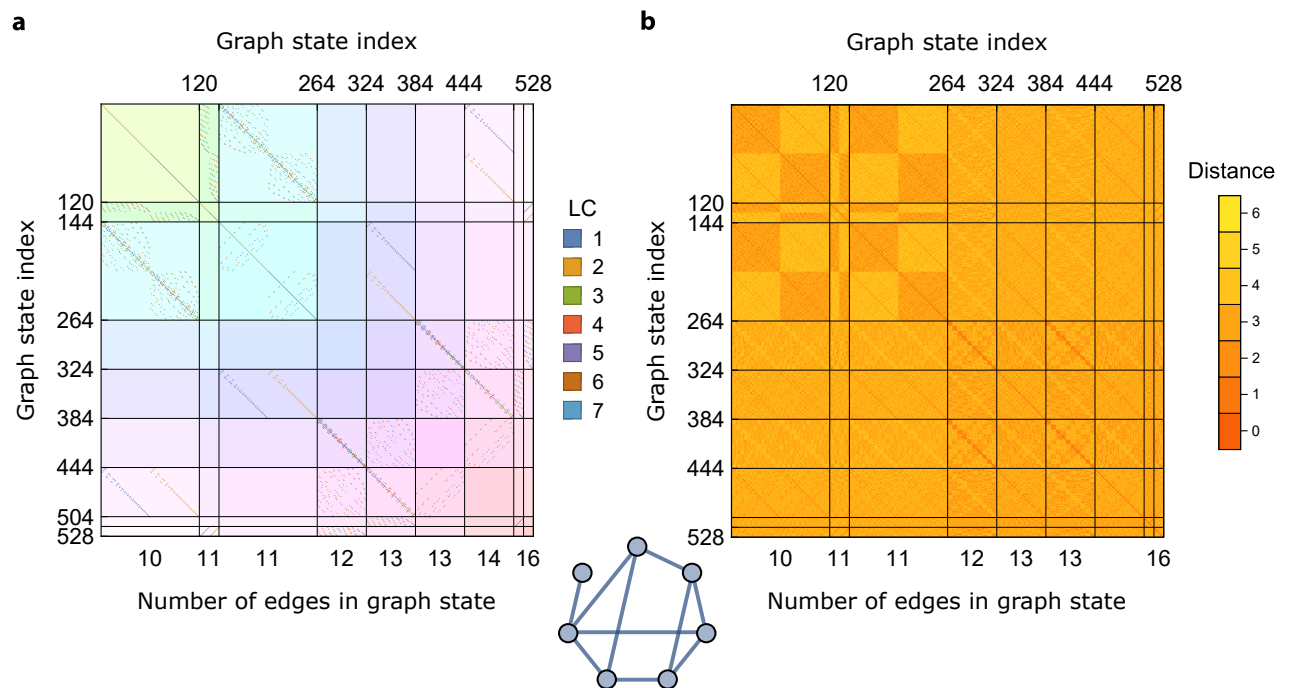


Appendix Figure 2: Local complementation orbit C_{18} . **a.** The orbit C_{18} . Here, graph state vertices which produce the same output when locally complemented are the same colour (see Section 2.3). **b.** The adjacency matrix of C_{18} . **c.** The distance matrix of C_{18} . Regions in the plot correspond to graph states which have the same number of edges.

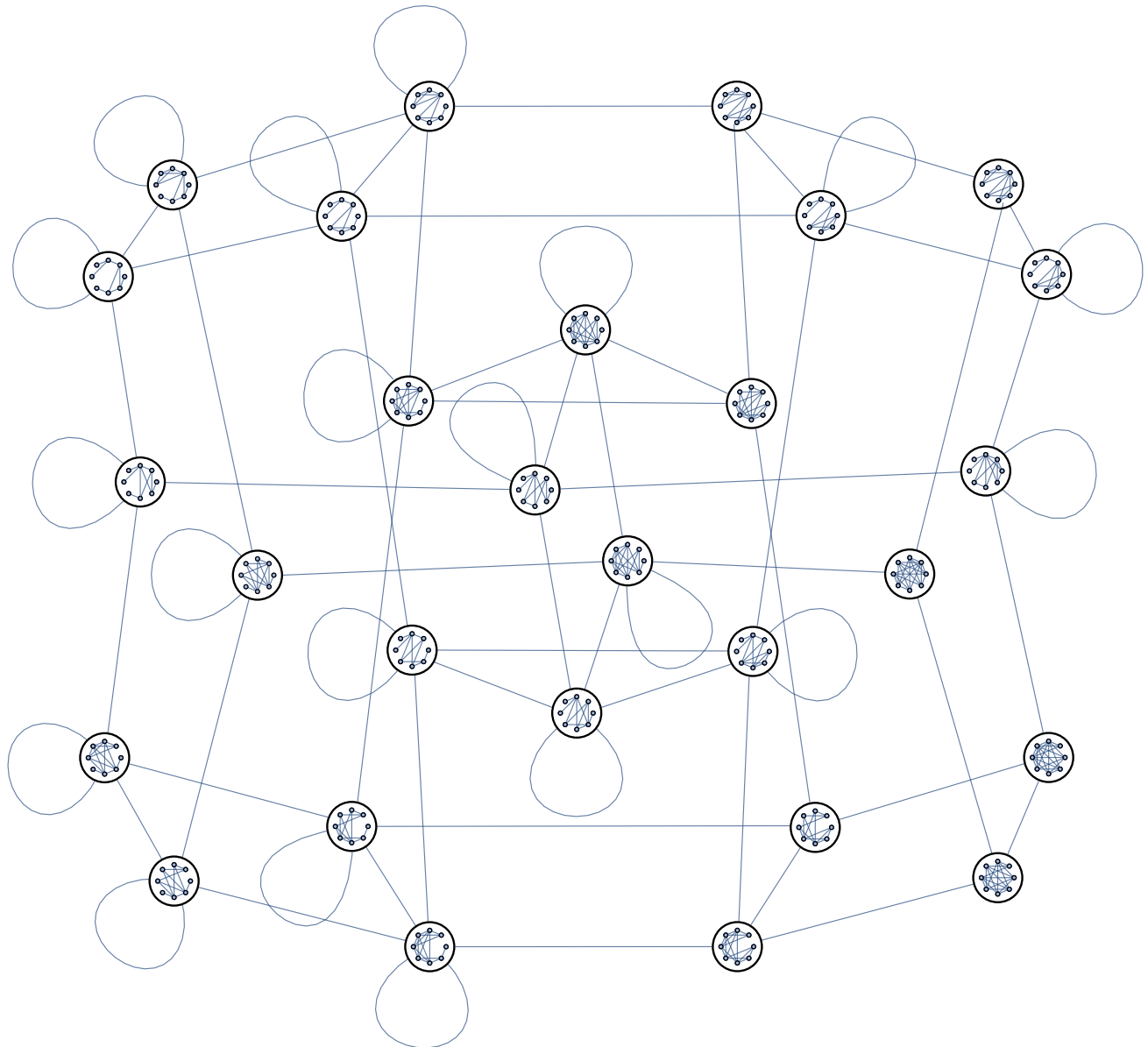
Appendix Figure 3: Orbit C_{196} .Appendix Figure 4: Orbit C_{289} .



Appendix Figure 5: Local complementation orbit 19. **a.** The orbit C_{19} . **b.** The adjacency matrix of L_{19} . **c.** The distance matrix of L_{19} . Regions in the plot correspond to graph states which are isomorphic. By separating regions corresponding to non-isomorphic graphs, we see that the orbit is composed of just two non-isomorphic graph states. These have 60 and 72 isomorphisms respectively.

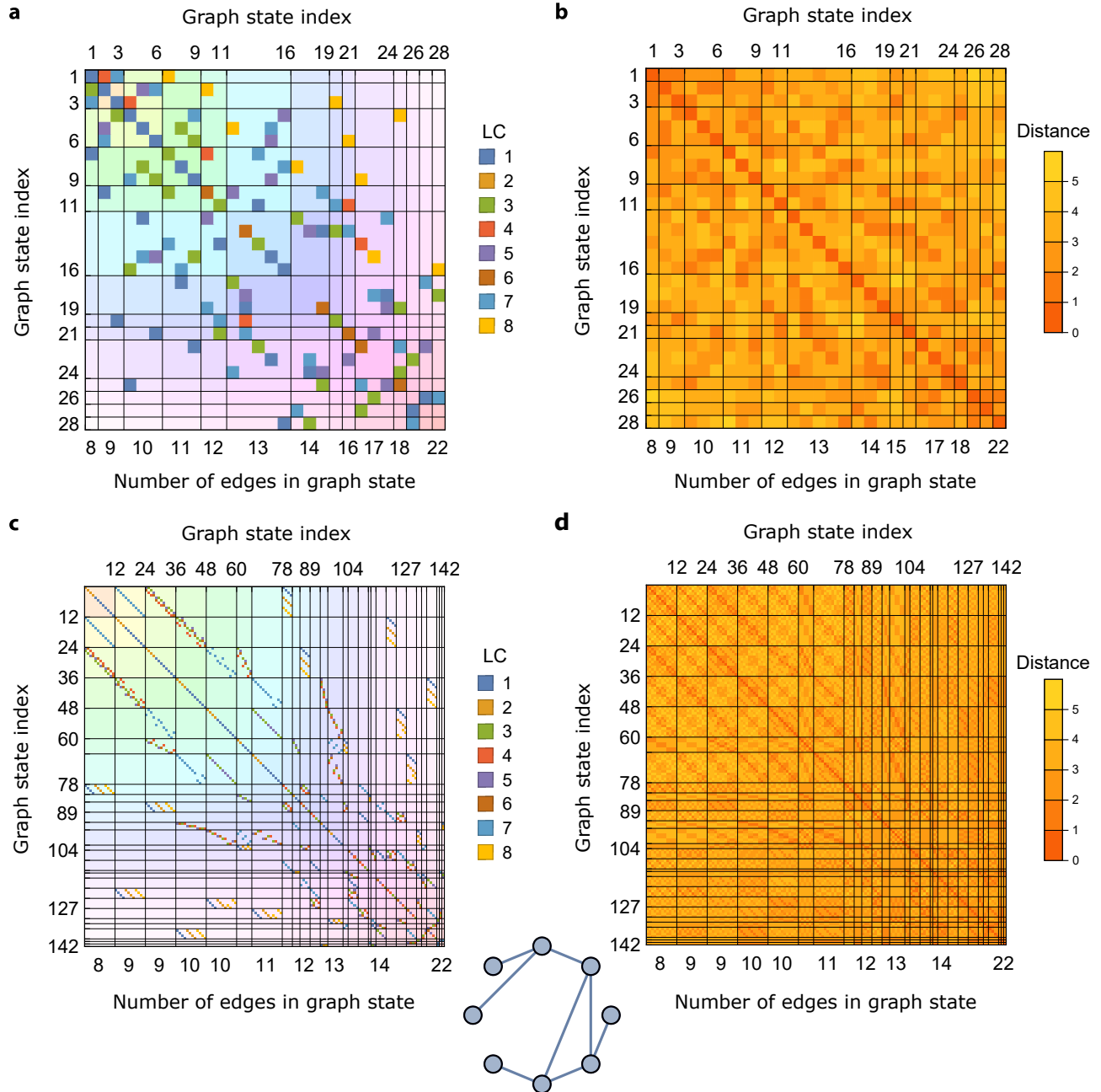


Appendix Figure 6: Local complementation orbit 45. **a.** The adjacency matrix of L_{45} . **b.** The distance matrix of L_{45} .

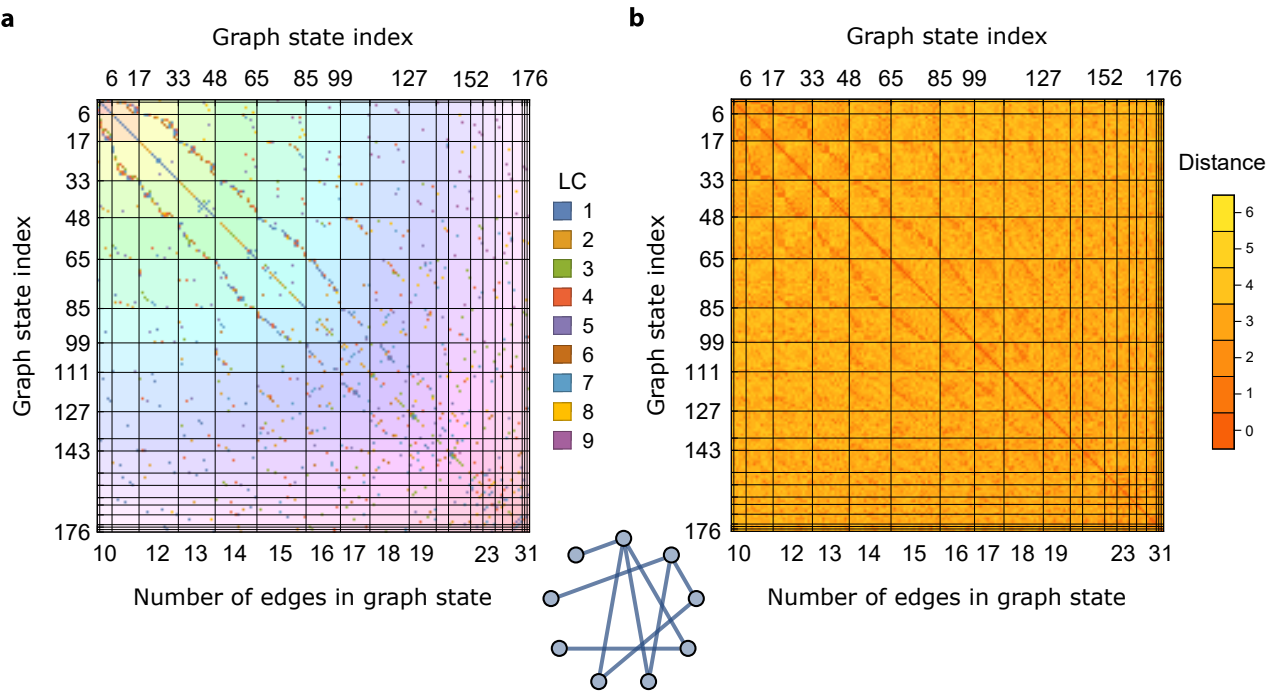


Appendix Figure 7: Orbit C_{78} . The adjacencies and distances matrices for for C_{78} and L_{78} are shown on the next page.

Appendix Figure 8: The orbit C_{78} .

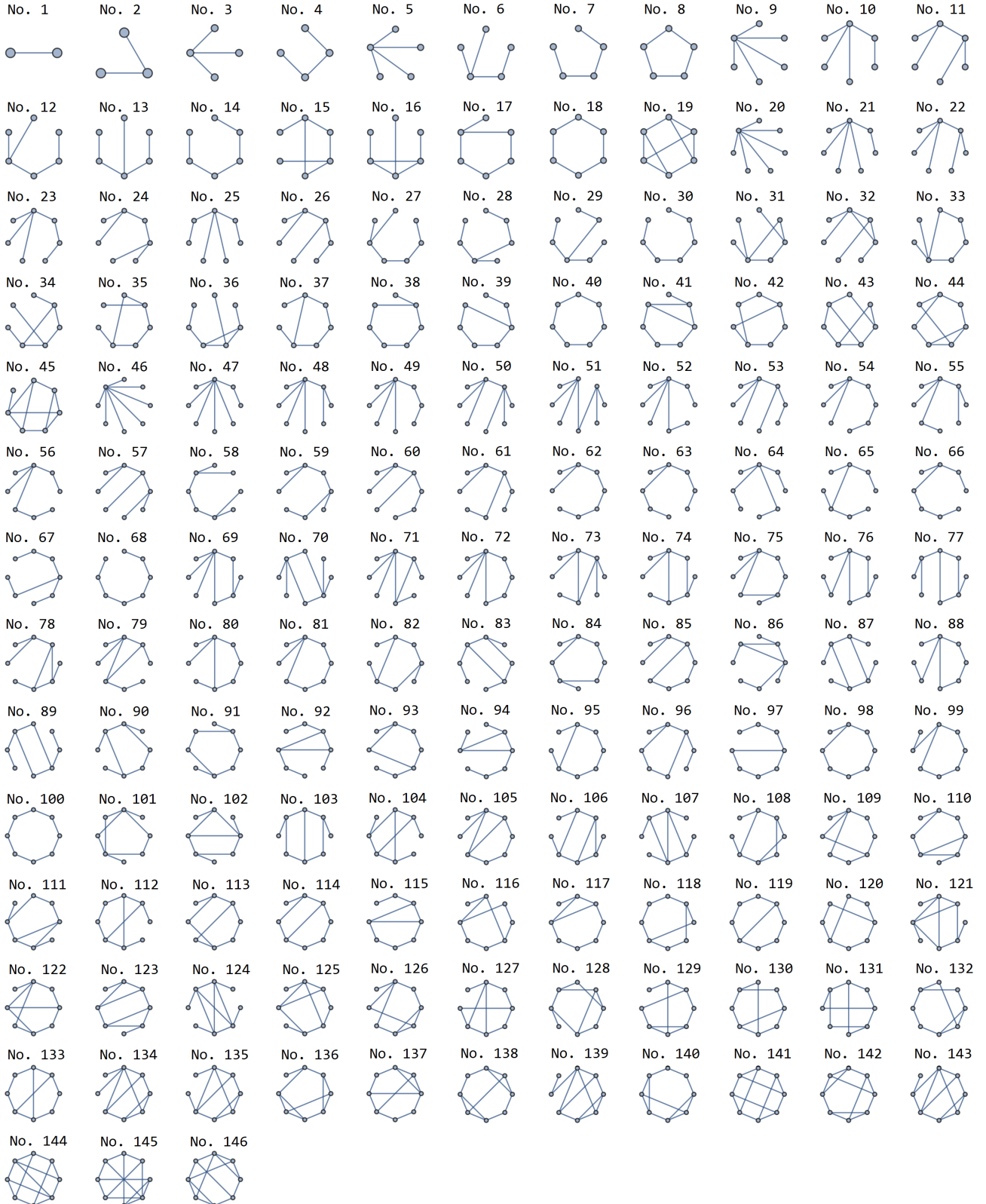


Appendix Figure 9: Comparison of L and C orbits for entanglement class 78. **a.** The adjacency matrix of C_{78} . **b.** The distance matrix of C_{78} . **c.** The adjacency matrix of L_{78} . **d.** The distance matrix of L_{78} . Regions in the plot correspond to graph states which have the same number of edges. Each demarcated region of L_{78} corresponds to a single graph state (vertex) of C_{78} .



Appendix Figure 10: C_{247} represented by its adjacency and distance matrices. **a.** The adjacency matrix. This matrix takes a value $A_{ij} = n$ where n is the index of the local complementation that links orbit vertices i and j . A different colour is used for each n . We demarcate regions of the plot which correspond to graph states with the same number of edges, and shade these in the same pastel shade. **b.** The distance matrix of C_{247} . This matrix takes a value $A_{ij} = n$ where n is the number of local complementations needed to transform graph state i into graph state j . The canonical representative graph state of the class is shown underneath.

2 Representative members of all graph state entanglement classes of $n < 9$ qubits



Appendix Figure 11: Canonical, minimal edge count representatives from each orbit up to and including 8 qubits. These are canonically indexed as in ref. 17